BMC Medical Imaging

RESEARCH

Open Access

A CT-based intratumoral and peritumoral radiomics nomogram for postoperative recurrence risk stratification in localized clear cell renal cell carcinoma

Xiaoxia Li[1†], Yi Guo[1†], Shunfa Huang[1†], Funan Wang[1], Chenchen Dai[2], Jianjun Zhou[1,2,3,4,5*] and Dengqiang Lin[6*]

Abstract

Objectives This study aimed to develop and validate a computed tomography (CT)-based intratumoral and peritumoral radiomics nomogram to improve the stratification of postoperative recurrence risk in patients with localized clear cell renal cell carcinoma (ccRCC).

Methods This two-center study included 447 patients with localized ccRCC. Patients from Center A were randomly split into a training set ($n=281$) and an internal validation set (IVS) ($n=114$) in a 7:3 ratio, while 52 patients from Center B formed the external validation set (EVS). Radiomics features from preoperative CT were obtained from the internal area of tumor (IAT), the internal and peritumoral areas of the tumor at 3 mm (IPAT 3 mm), and 5 mm (IPAT 5 mm). The least absolute shrinkage and selection operator (LASSO) Cox regression was used to construct a radiomics score to develop radiomics model (RM). A clinical model (CM) was also established using significant clinical factors. Furthermore, a fusion model (FM) was developed by integrating independent predictors from both clinical factors and the radiomics score (Radscore) through multivariate Cox proportional hazards regression. Model performance was assessed with Kaplan-Meier curves, time-dependent area under the curve (time-AUC), Harrell's concordance index (C-index), and decision curve analysis (DCA).

Results Compared to both the IAT model and the IPAT 3 mm model, the IPAT 5 mm radiomics model demonstrated superior predictive performance for tumor recurrence (C-index: 0.924 vs. 0.915–0.923 in the IVS; 0.952 vs. 0.920–0.944 in the EVS). Therefore, the IPAT 5 mm radiomics score was incorporated into the development of the fusion model. The FM exhibited outstanding predictive accuracy, achieving a C-index of 0.938 in the IVS, significantly outperforming

†Xiaoxia Li, Yi Guo and Shunfa Huang contributed equally to this work and share first authorship.

Jianjun Zhou and Dengqiang Lin contributed equally to this work and listed as co-corresponding authors.

*Correspondence:
Jianjun Zhou
zhoujianjunzs@126.com
Dengqiang Lin
153365650@qq.com

Full list of author information is available at the end of the article

the CM (0.889, $P=0.03$). Notably, in the EVS, the RM surpassed both the CM and FM (C-index: 0.952 vs. 0.904–0.940, $P>0.05$). Furthermore, decision curve analysis indicated that the FM provided the highest net clinical benefit in the IVS, while both the FM and RM demonstrated substantially greater net benefit than the CM in the EVS.

Conclusions The radiomics model and the fusion model, which integrate both intratumoral and peritumoral features, offer accurate prediction of recurrence risk in patients with localized ccRCC. These models have the potential to aid in personalized treatment planning, optimized surveillance strategies, and treatment strategies for patients with clear cell renal cell carcinoma.

Keywords Computed tomography, Radiomics, Recurrence, Clear cell renal cell carcinoma

Introduction

Clear cell renal cell carcinoma (ccRCC) is the most common type of kidney cancer, accounting for approximately 75-80% of diagnosed cases [1]. The incidence of ccRCC has been increasing in both males and females over the past few decades [2]. While most patients with localized ccRCC have slow-growing tumors that are not life-threatening, about 20–30% of patients experience disease recurrence and metastasis after complete tumor removal. The prognosis for patients with metastatic ccRCC is very poor. A recent study has suggested that adjuvant-targeted therapy may only be beneficial for a limited number of patients with non-metastatic ccRCC [3]. However, subjecting all ccRCC patients to potentially harmful adjuvant-targeted therapy would result in unnecessary medical interventions [4]. Therefore, it is crucial to improve the selection process for patients based on their risk of recurrence. This would ensure that only those with a favorable risk-to-benefit ratio for adjuvant immunotherapy receive the treatment.

Traditionally, recurrence risk assessment in ccRCC has been based on TNM classification and nuclear grade. However, these factors alone offer limited prognostic accuracy. To enhance predictive performance, various prognostic models [5–7] now integrate multiple indicators, with the Stage, Size, Grade, and Necrosis (SSIGN) model being one of the most widely used. By incorporating tumor size, nuclear grade, and histological necrosis alongside TNM staging, SSIGN improves survival prediction in ccRCC. Nevertheless, significant survival variations still exist among patients within the same SSIGN category, highlighting the need for further refinement. Moreover, SSIGN primarily relies on pathological features obtained through multi-site sampling of key tumor regions. This approach not only risks omitting comprehensive tumor information but is also impractical for preoperative assessment. Therefore, identifying novel prognostic factors remains an urgent priority.

Radiomics is an emerging technique that extracts a wide range of quantitative imaging features through computerized analysis [8, 9]. It has demonstrated potential in differentiating benign from malignant renal tumors [10], identifying subtypes [11, 12], assessing tumor grade and stage [13–16] and predicting survival outcomes [17, 18]. A recent multicenter study [19] employed radiomics to evaluate recurrence and metastasis in localized renal cell carcinoma, revealing that integrating radiomics with existing prognostic models improved predictive performance (C-index: 0.74–0.78). Similar findings were reported in a single-center study of 453 patients [20]. However, the accuracy of these models in predicting recurrence-free survival (RFS) remains limited. Notably, prior studies have focused solely on intratumoral radiomics while overlooking peritumoral features. Growing evidence suggests that peritumoral imaging plays a crucial role in tumor diagnosis, grading, and prognosis by providing insights into the tumor's surrounding microenvironment [21–23]. Peritumoral radiomics has been utilized to predict clinical outcomes in lung [21], cervical [24] and breast cancers [25]. Our previous study [26] demonstrated the value of combining peritumoral and intratumoral radiomics for tumor grade prediction. However, the potential of integrating both peritumoral and intratumoral radiomics for survival outcome prediction remains largely unexplored.

This study aimed to develop and validate a CT-based intratumoral and peritumoral radiomics nomogram to improve the stratification of postoperative recurrence risk in patients with localized clear cell renal cell carcinoma (ccRCC).

Methods

Patients

This retrospective study was conducted in accordance with the ethical guidelines of the Declaration of Helsinki and received approval from our hospital's ethics committee, with a waiver for informed consent. Data were collected from the medical records of 447 patients with clear cell renal cell carcinoma (ccRCC) who underwent radical or partial nephrectomy between January 2015 and June 2019. The inclusion and exclusion criteria are detailed in Fig. 1. Patients were randomly assigned to the training set and internal validation set (IVS) in a 7:3 ratio. Additionally, 52 patients from our branch hospital, meeting the same inclusion and exclusion criteria, were included in the external validation set (EVS).

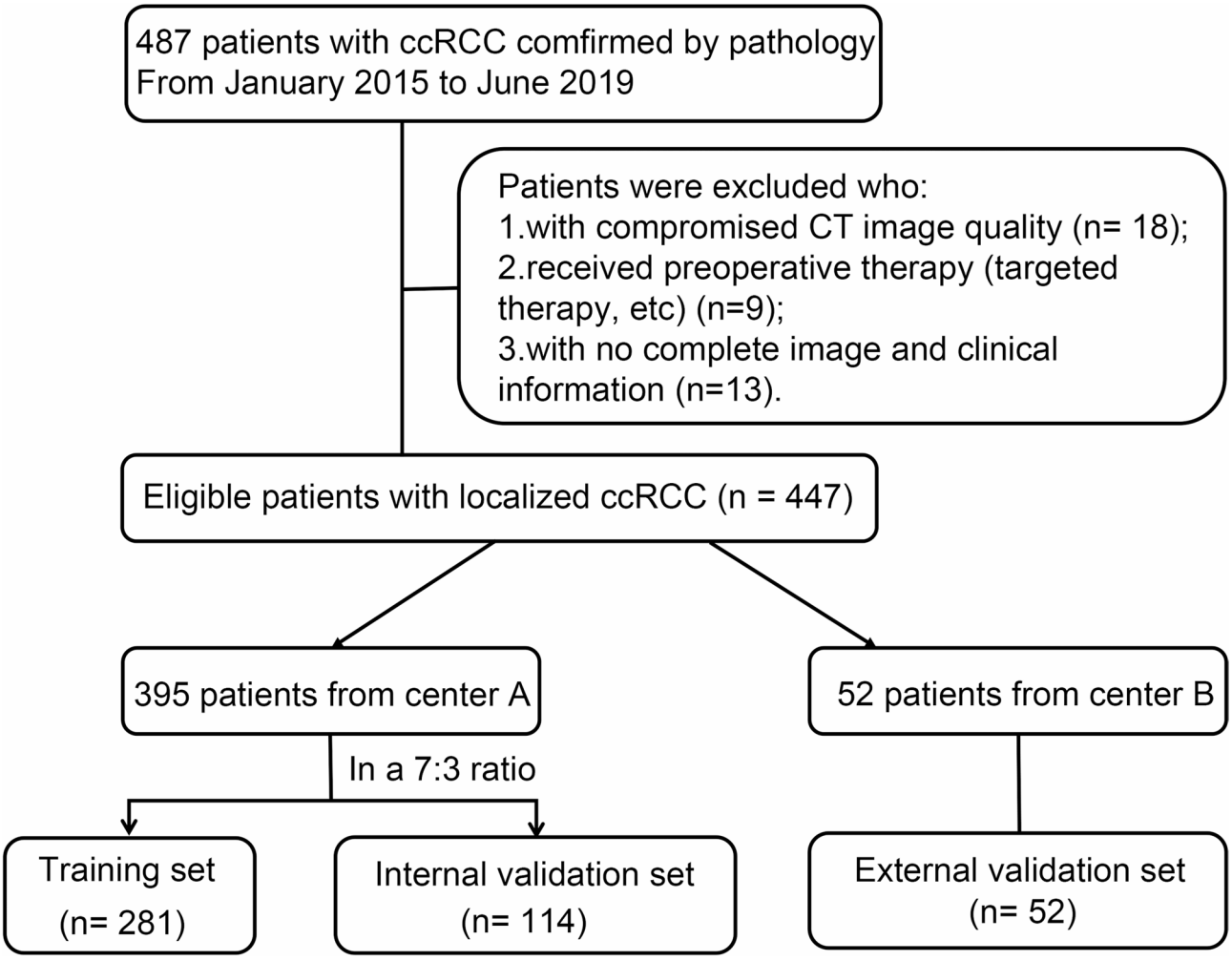

Fig. 1 Flowchart illustrating the patient exclusion pathway

Recurrence-free survival (RFS) was defined as the time from surgery to recurrence, death, or last follow-up. For each patient, demographic and clinical parameters were collected, including age, sex, Eastern Cooperative Oncology Group Performance Status (ECOG-PS), nephrectomy type, tumor size, the International Society of Urological Pathology (ISUP) grade, pathological T and N stage, tumor necrosis, and the presence of sarcomatoid differentiation.

Image acquisition and tumor segmentation

All patients underwent a preoperative contrast-enhanced CT scan using either a 16-detector or 64-detector scanner. Arterial-phase CT images of ccRCC patients were analyzed. Detailed CT parameters are provided in Appendix S1. Information regarding tumor segmentation is outlined in Appendix S2 and illustrated in Fig. 2.

Radiomics feature extraction

Before conducting feature extraction, the CT images underwent preprocessing procedures that included resampling and standardization to ensure replicable results. Pyradiomics v3.0.1 package (https://pypi.org/project/pyradiomics/) was utilized to extract radiomic features from the regions of interest (ROIs). Details regarding the extracted features are presented in Appendix S3.

Reproducibility analysis

Initially, the z-score method was applied to standardize radiomic features. To evaluate feature reproducibility, a set of 30 randomly selected CT images was analyzed. Interobserver repeatability was assessed by comparing the delineations of the intratumoral area of tumor(IAT), intratumoral and peritumoral 3 mm area (IPAT 3 mm), and intratumoral and peritumoral 5 mm area (IPAT 5 mm) performed independently by Radiologist 1 (L.X.) and Radiologist 2 (G.Y.) within the same timeframe. Intraobserver repeatability was further evaluated by

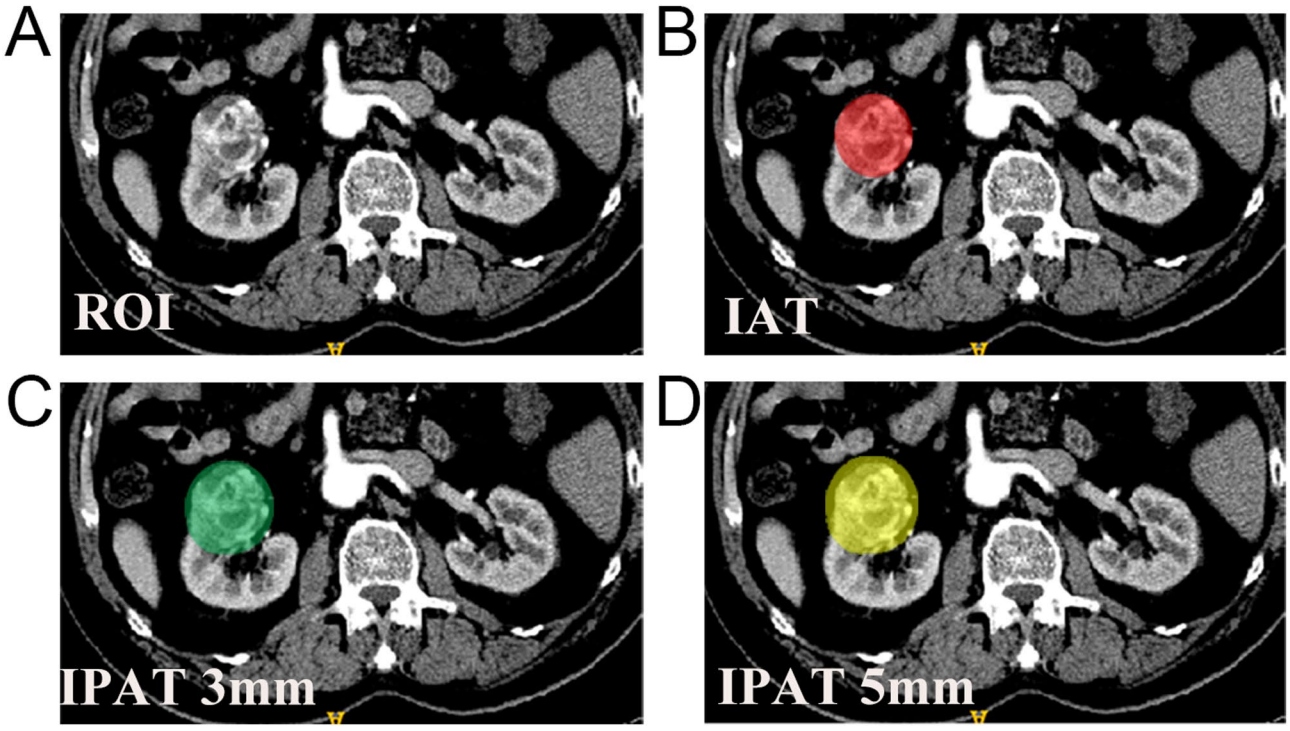

Fig. 2 Tumor segmentation across different regions. (**A**) Original ROI, (**B**) IAT ROI, (**C**) IPAT 3 mm ROI, (**D**) IPAT 5 mm ROI

having Radiologist 1 repeat the delineation after one month. Both radiologists remained blinded to the pathological findings throughout the evaluation. Inter- and intraobserver reliability was assessed using intraclass correlation coefficients (ICCs), categorized as poor (ICC < 0.5), moderate (ICC 0.5–0.75), good (ICC 0.75–0.90), or excellent (ICC > 0.90). An ICC greater than 0.75 was considered to indicate high consistency [27, 28].

Feature selection and radiomics nomogram construction

After selecting the remaining features with an ICC greater than 0.75, univariate Cox proportional hazards regression (CPHR) analysis was performed to identify radiomic features significantly associated with recurrence-free survival (RFS). Features with $p < 0.05$ in the univariate analysis was further refined using the least absolute shrinkage and selection operator (LASSO) Cox method. A 10-fold cross-validation was conducted to determine the optimal λ, selecting the value that minimized cross-validation error. Features with non-zero coefficients from the LASSO algorithm were then used to construct the radiomics models (RM) for tumor recurrence prediction and were aggregated into a radiomics score (Radscore).

To evaluate the discriminative performance of the radiomics signature, the Wilcoxon test was employed to compare Radscores between the recurrence and no-recurrence groups. In parallel, a clinical model (CM) was developed by identifying independent clinical predictors of tumor recurrence through both univariable and multivariable Cox analyses. Finally, a fusion model (FM) was established by integrating the Radscore from the best-performing RM with the independent clinical predictors.

Model evaluation and survival analysis

The performance of the models was evaluated using Harrell's concordance index (C-index) and the time-dependent area under the curve (time-AUC) of receiver operating characteristic (ROC) curves. A calibration curve was plotted to assess the model's agreement between predicted and actual outcomes. To evaluate the clinical utility of the model, decision curve analysis (DCA) was performed, quantifying the net benefits across varying threshold probabilities. Additionally, by using X-Tile software, the optimal cut points of the scores calculated by nomogram-predicted were identified, and the patients were categorized as high-, and low-risk groups. The Kaplan-Meier method was performed and the log-rank test was applied to determine the statistical significance of differences between these groups.

Comparison with the existing prognostic models

To assess predictive performance, we compared the effectiveness of the nomogram with that of the SSIGN model. Detailed descriptions of the calculation procedures for SSIGN score can be found in Appendix S4.

Statistical analysis

Continuous variables were expressed as mean ± standard deviation (SD) or median (interquartile range, IQR), depending on their distribution. For normally distributed data, comparisons between groups were performed using the independent t-test; for non-normally distributed data, the Mann-Whitney U test was used. Categorical variables were compared using the chi-square test or Fisher's exact test. To identify independent predictors for tumor recurrence, we performed both univariable and multivariable Cox analyses. Variables demonstrating p-values < 0.05 in the univariate analysis were included in the multivariate analysis, which employed backward stepwise selection based on the Akaike Information Criterion (AIC). Statistical analyses were conducted using SPSS v.20.0 and R software, version 4.2.0. Two-sided p-values < 0.05 were considered statistically significant.

Results

Patients

The characteristics of ccRCC patients are summarized in Table 1, detailing the distribution across the training set (TS) ($n = 281$), internal validation set (IVS) ($n = 114$), and external validation set (EVS) ($n = 52$). No significant differences were found in clinical data between the TS and IVS, except for sex, while the only notable difference between the two centers was the follow-up duration. The overall median recurrence-free survival (RFS) was 46.5 months, with 46 out of 447 patients (10.3%) experiencing recurrence after complete surgical resection. The median RFS was 48.1 months (IQR: 35.0–63.1) in the TS, 48.0 months (IQR: 34.7–64.4) in the IVS, and 28.5 months (IQR: 20–44) in the EVS. Recurrence rates were 9.96% (28/281) in the TS, 11.4% (13/114) in the IVS, and 9.6% (5/52) in the EVS.

Table 1 Characteristics of patients

Clinical factors	Center A ($n = 395$)	Training Set ($n = 281$)	Internal validation Set ($n = 114$)	P^* value	Center B External validation Set ($n = 52$)	$P^{\#}$ value
Age (years)	60.0(53.0; 67.0)	59.0(53.0; 67.0)	60.0(51.2; 65.0)	0.211	58(49; 69.3)	0.377
Tumor-size (cm)	4.0 (2.9; 5.5)	4.1 (2.8; 5.5)	3.9 (3.1; 5.3)	0.980	3.5 (2.5;4.9)	0.084
Sex				0.001*		0.203
Female	130(32.9)	107 (38.1)	23 (20.2)		12 (23.1)	
Male	265 (67.1)	174 (61.9)	91 (79.8)		40 (76.9)	
ISUP grade				0.926		0.168
I	14 (3.5)	11 (3.9)	3 (2.6)		3 (5.8)	
II	314 (79.5)	223 (79.4)	91 (79.9)		44 (84.6)	
III	58 (14.7)	41 (14.6)	17 (14.9)		3 (5.8)	
IV	9 (2.3)	6 (2.1)	3 (2.6)		2 (3.8)	
T stage				0.08		0.574
T1	323 (81.8)	234 (83.3)	89 (78.0)		46 (88.4)	
T2	42 (10.6)	31 (11.0)	11 (9.7)		3 (5.8)	
T3	30 (7.6)	16 (5.7)	14 (12.3)		3 (5.8)	
N stage				0.494		1.000
N0/x	393 (99.5)	280 (99.6)	113 (99.1)		52 (100)	
N1	2 (0.5)	1 (0.4)	1 (0.9)		0 (0)	
Tumor Necrosis				0.417		0.785
Absent	362 (91.6)	255 (90.7)	107 (93.9)		49 (94.2)	
Present	33 (8.4)	26 (9.3)	7 (6.1)		3 (5.8)	
Nephrectomy type				0.787		0.463
Radical	238 (60.3)	171 (60.9)	67 (58.8)		28 (53.9)	
Patial	157 (39.7)	110 (39.1)	47 (41.2)		24 (46.1)	
ECOG-PS						0.166
0 score	341 (86.3)	239 (85.1)	102 (89.5)	0.319	49 (94.2)	
> 0 score	54 (13.7)	42 (14.9)	12 (10.5)		3 (5.8)	
Recurrence				0.808		1.000
Absent	354 (89.6)	253 (89.1)	101 (88.6)		47 (90.4)	
Present	41 (10.4)	28 (9.96)	13 (11.4)		5 (9.6)	
Follow-up time	48.1(34.9; 63.1)	48.1(35.0; 63.1)	48.0(34.7; 64.4)	0.967	28.5(20.0;44.0)	< 0.001

Quantitative variables were expressed as median (interquartile range) and analyzed by Student's t test or Mann-Whiney U test. For qualitative variables, percentages or frequencies were calculated and a χ^2 test. *Significant results. P^* was compared between the training set and the internal validation set, while $P^{\#}$ was based on the comparison between center A and B

ISUP grade, the International Society of Urological Pathology grading system. ECOG-PS, Eastern Cooperative Oncology Group Performance Status

Radiomics feature selection

A total of 1,834 radiomic features were extracted from each ROI of the IAT, IPAT 3 mm, and IPAT 5 mm. All extracted features were standardized using the Z-score method. The reproducibility of these features was excellent, with high consistency observed in 86.0% (1579/1834) of IAT features, 92.4% (1694/1834) of IPAT 3 mm features, and 91.0% (1669/1834) of IPAT 5 mm features. Initially, univariate Cox proportional hazards regression (CPHR) analysis was performed to assess the association between the remaining radiomics features and RFS, resulting in the selection of 896 features for IAT ROIs, 984 features for IPAT 3 mm ROIs, and 1,002 features for IPAT 5 mm ROIs. These selected features were then subjected to least absolute shrinkage and selection operator (LASSO) regression analysis to remove redundant and irrelevant variables, leading to the construction of the radiomics models (RM), as illustrated in Fig. 3. Ultimately, five, five, and six optimal radiomics features were retained for the IAT ROIs, IPAT 3 mm ROIs, and IPAT 5 mm ROIs, respectively. The specific Radscore formulas for the three radiomics models are provided in Appendix S5.

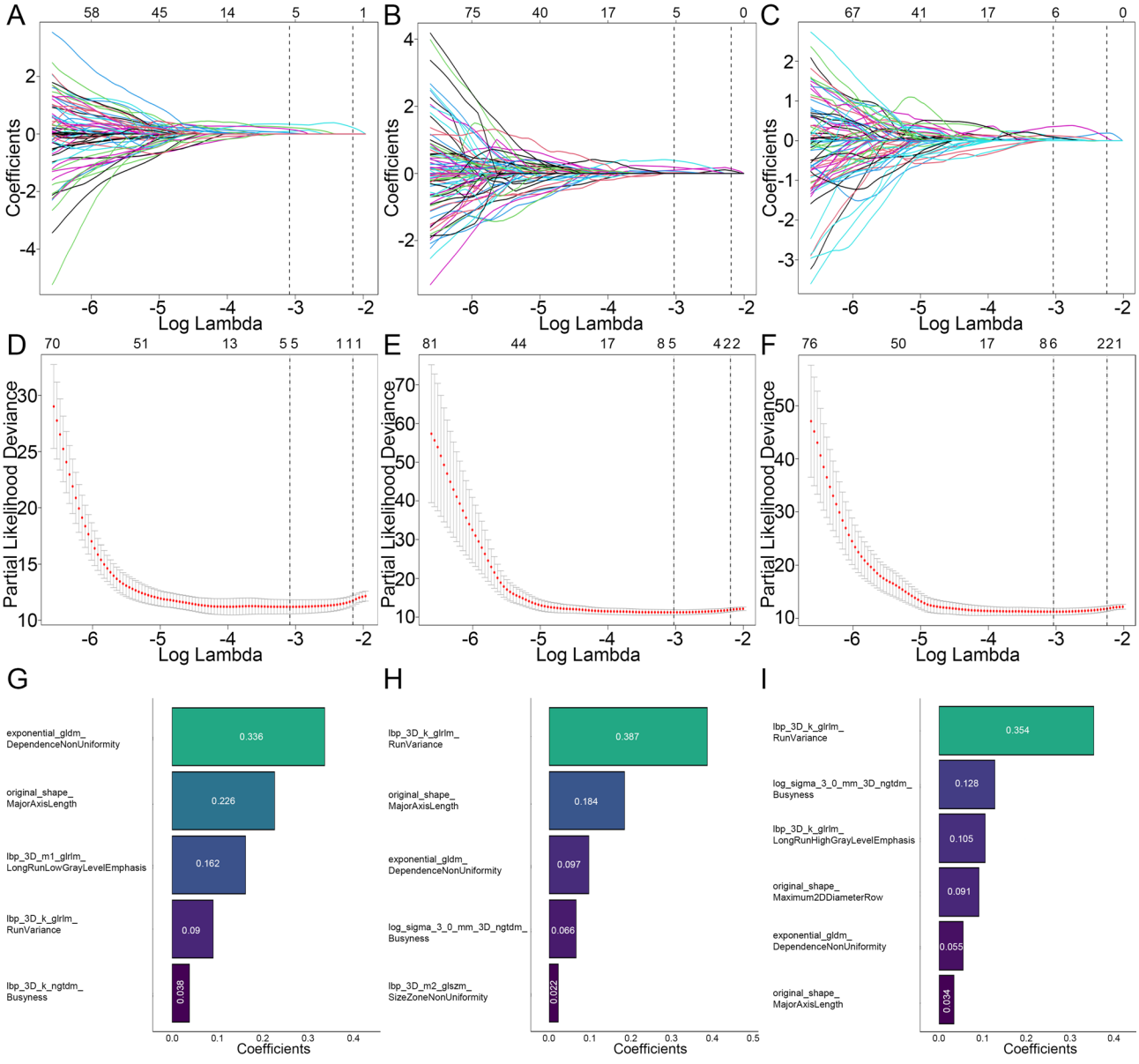

Fig. 3 Screening path of the least absolute shrinkage and selection operator (LASSO) regression model: (**A**) IAT model, (**B**) IPAT 3 mm model, (**C**) IPAT 5 mm model. Penalty parameter (log lambda) in the LASSO regression model: (**D**) IAT model, (**E**) IPAT 3 mm model, (**F**) IPAT 5 mm model. Retained radiomics features and corresponding coefficients of different models after dimensionality reduction by LASSO regression: (**G**) IAT model, (**H**) IPAT 3 mm model, (**I**) IPAT 5 mm model

Radiomics model analysis

Compared to both the IAT model and the IPAT 3 mm model, the IPAT 5 mm radiomics model demonstrated relatively superior predictive performance for tumor recurrence (C-index: 0.924 vs. 0.915–0.923, $P = 0.539$–0.80, in the IVS; 0.952 vs. 0.920–0.944, $P = 0.23$–0.608 in the EVS) (Table S1). The Wilcoxon test further revealed that the Radscore derived from the IPAT 5 mm model was significantly higher in patients with recurrence than in those without across all datasets ($P < 0.05$) (Fig. S1). Accordingly, the IPAT 5 mm model was selected for constructing the nomogram to predict tumor recurrence.

Radiomics nomogram construction

A multivariate cox regression analysis was performed to determine the factors that independently predicted ccRCC recurrence, namely patient age (HR = 1.07; 95% CI = 1.02–1.122, $P = 0.006$), histologic grade (HR = 2.645; 95% CI = 1.149–6.089, $P = 0.022$), p-T stage (HR = 2.254; 95% CI = 1.218–4.171, $P = 0.01$), p-N stage (HR = 232.85; 95% CI = 20.2-2683.52, $P < 0.001$) (Table 2), and Radscore gained from IPAT 5 mm model (HR = 6.061; 95% CI = 2.349–15.64, $P < 0.001$). To create a fusion model (FM), a nomogram was developed that incorporated both the PAT 5-mm radiomics signature and independent features (Fig. 4A). All independent clinical features including patient age, histologic grade, p-T stage, and p-N stage were entered into the Cox-regression model to develop the clinical model (CM).

Table 2 Univariable and multivariable Cox regression analysis for association of variables with recurrence-free survival

	Univariable cox regression		Multivariable cox regression	
	HR (95% CI)	P value	HR (95% CI)	P value
Age, years	1.061 (1.021–1.103)	0.003	1.07 (1.02–1.122)	0.006
Sex (female as ref)	1.867 (0.794–4.393)	0.153		
Tumor size,cm	1.601 (1.369–1.873)	< 0.001		
Nephrectomytype (Radical as ref)	0.116 (0.028–0.489)	0.003		
ECOG-PS (0 as ref)	2.156 (0.916–5.077)	0.079		
ISUP grade (III-IV vs I-II)	4.222 (1.997–8.928)	< 0.001	2.645 (1.149–6.089)	0.022
T stage (T3 vs T2 vs T1)	4.473 (2.952–6.779)	< 0.001	2.254 (1.218–4.171)	0.01
N stage (N1 vs N0/x)	34.22 (4.28-273.61)	< 0.001	232.85(20.2-2683.52)	< 0.001
RM_{5mm}-Radscore	4.255 (2.849–6.355)	< 0.001	6.061 (2.349–15.64)	< 0.001

RM_{5mm}-Radscore, the radscore gained from IPAT 5 mm model. ISUP grade, the International Society of Urological Pathology grading system. ECOG-PS, Eastern Cooperative Oncology Group Performance Status

Predictive performance of the model and survival analysis

The FM exhibited outstanding predictive accuracy, achieving a C-index of 0.938 in the IVS, which was significantly higher than that of the CM (C-index: 0.889, $P = 0.03$) and demonstrated a trend toward superior performance compared to the RM (C-index: 0.924, $P = 0.37$). Interestingly, in the EVS, the RM outperformed both the CM and FM (C-index: 0.952 vs. 0.904–0.940, $P > 0.05$) (Table 3). The time-AUC curve further supported these findings (Fig. 4B-D). Additionally, the predictive model demonstrated good agreement between the predicted and actual RFS probabilities at 1, 3, and 5 years, as validated by the calibration curve (Fig. S2). Decision curve analysis (DCA) revealed that the FM provided a greater net benefit than the CM and RM for predicting RFS at 5 years in both the TS and IVS, while in the EVS, both the FM and RM exhibited substantially higher net benefits compared to the CM (Fig. 4E-G). Finally, Kaplan-Meier survival curves indicated that RFS, as determined by the nomogram-predicted risk stratification, was significantly worse for high-risk patients than for low-risk patients across the TS, IVS, and EVS (Fig. 5A-C).

Comparison with existing model

The FM exhibited a higher C-index than the SSIGN model in the internal validation set (C-index: 0.938 vs. 0.886, $P < 0.001$). In the external validation set, the SSIGN model slightly outperformed FM, but the difference was not statistically significant (C-index: 0.912 vs. 0.904, $P = 0.687$) (Table S2).

Stratified analysis of the nomogram in subgroups

The Kaplan-Meier survival curves clearly indicated significant differences in recurrence-free survival (RFS) among the different nomogram-predictive risks in patients categorized by SSIGN-based risk, ISUP grade, and those with tumors larger than 4 cm, while no significant differences were observed in the subgroup with tumors smaller than 4 cm (Fig. S3).

Discussion

This retrospective cohort study developed a radiomics-based nomogram that integrates intratumoral and peritumoral radiomic features with key clinicopathological factors, offering a noninvasive tool for personalized recurrence-free survival (RFS) prediction in clear cell renal cell carcinoma (ccRCC). In the internal validation cohort, the fusion model exhibited superior prognostic performance (C-index: 0.938, 95% CI: 0.905–0.971),

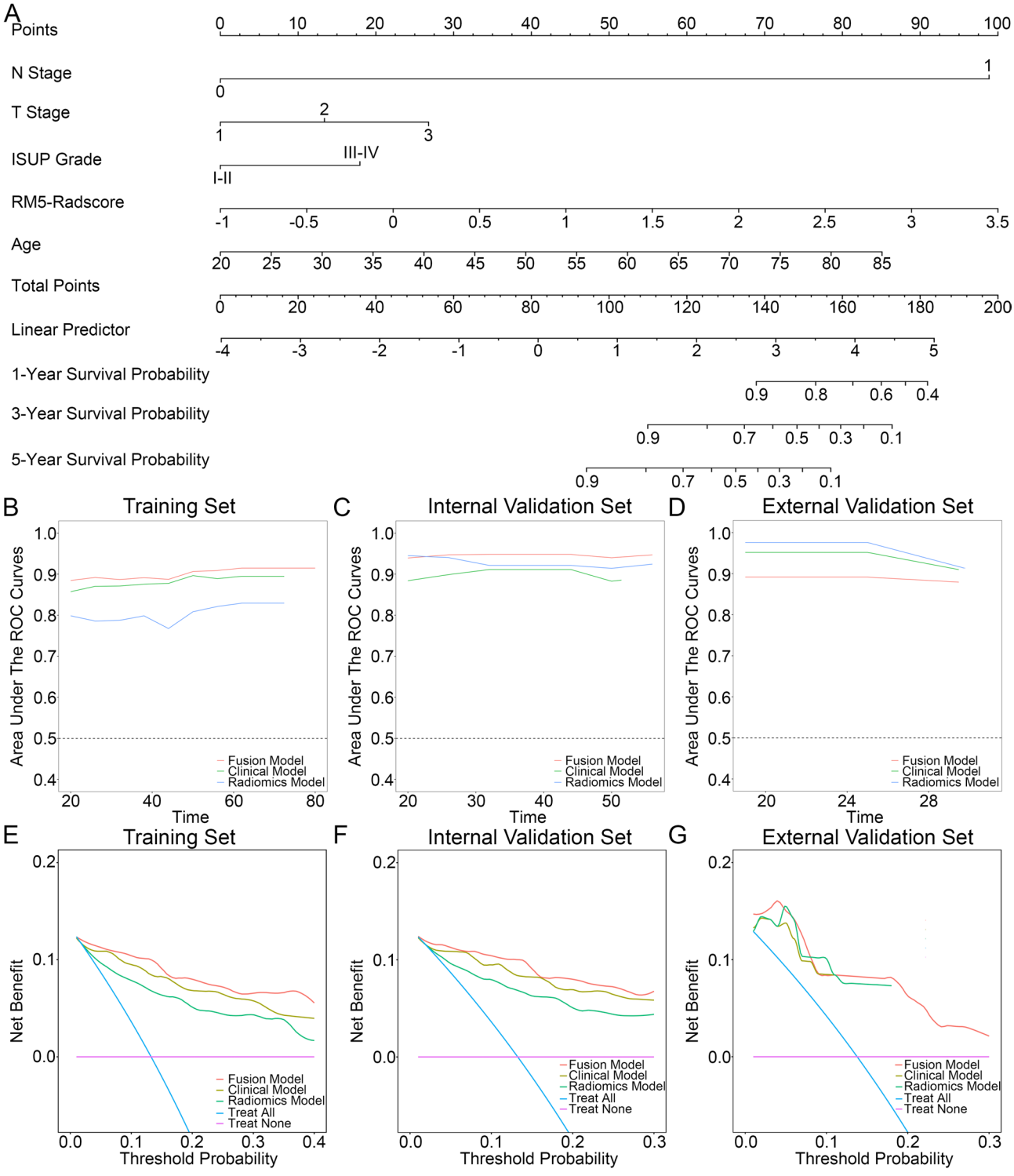

Fig. 4 (**A**) Illustration of the nomogram (fusion model). Predictive performance of the models assessed using the time-AUC curve for: (**B**) training set, (**C**) internal validation set, (**D**) external validation set. Decision curve analysis of the fusion model, clinical model, and radiomics model for predicting RFS at: (**E**) 5 years in the training set, (**F**) 5 years in the internal validation set, and (**G**) 3 years in the external validation set

Table 3 Performance of clinical model, radiomics model, and fusion model

	Training set			Internal validation set			External validation set		
	C-index	95% CI	P value	C-index	95% CI	P value	C-index	95% CI	P value
Fusion model	0.897	0.853–0.941	-	0.938	0.905–0.971	-	0.904	0.819–0.989	-
Clinical model	0.880	0.834–0.927	0.272	0.889	0.830–0.949	0.037	0.940	0.874–1.006	0.271
Radiomics model	0.799	0.720–0.876	0.01	0.923	0.878–0.969	0.379	0.952	0.887–1.017	0.229

P value was compared with Fusion model

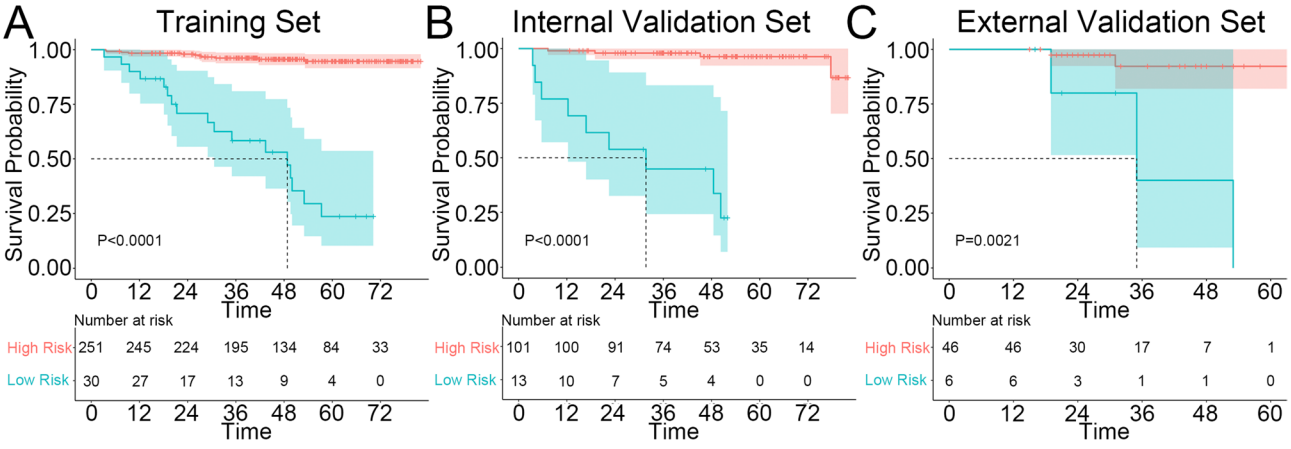

Fig. 5 Kaplan-Meier survival curves for the nomogram in: (**A**) training set, (**B**) internal validation set, and (**C**) external validation set

surpassing both the radiomics model (C-index: 0.924, $P = 0.379$) and the clinical model (C-index: 0.889, $P = 0.037$). However, in the external validation cohort, the radiomics model demonstrated the highest predictive accuracy (C-index: 0.952), outperforming both the clinical and fusion models (C-index: 0.904–0.940, all $P > 0.05$). Additionally, Kaplan-Meier survival curves indicated significant differences in RFS across distinct risk categories predicted by the nomogram in all cohorts.

Radiomic studies have highlighted the prognostic value of peritumoral regions in oncology [23, 29], likely due to tumor cell migration and microenvironmental changes. These regions provide additional insights into tumor heterogeneity beyond intratumoral features. In this study, we integrated peri- and intratumoral features into our radiomics model, which showed a slight performance improvement over the intratumoral-only model (C-index: 0.923–0.924 vs. 0.915 in the IVS; 0.944–0.952 vs. 0.920 in the EVS, all $P > 0.05$), though statistical significance was not reached. The limited incremental value of peritumoral features may be attributed to two factors. First, our automated segmentation protocol, which extends from the tumor core to the peritumoral region, may have caused substantial feature overlap, reducing performance differentiation. Second, the sample size may have been insufficient to detect subtle performance variations. Despite the lack of statistical significance, the observed trend of improved performance with peritumoral expansion suggests its potential prognostic value in predicting ccRCC recurrence. Future studies will explore larger multicenter cohorts to enhance statistical power and refine pure peritumoral models through optimized segmentation strategies.

Our study demonstrates that the proposed nomogram outperforms the clinical model in prognostic accuracy. In the internal validation cohort, the nomogram achieved a significantly higher concordance index (C-index) than the clinical model (0.938 vs. 0.889, $P = 0.037$). Moreover, in the external validation cohort, the radiomics-based model further improved predictive accuracy compared to the nomogram (0.952 vs. 0.904), although this difference did not reach statistical significance ($P = 0.229$). This finding underscores the potential of radiomics in enhancing prognostic assessment, as it extracts high-dimensional imaging features that may capture tumor heterogeneity [19, 30–32]. Decision curve analysis (DCA) further supports the clinical utility of both the nomogram and radiomics models. Compared to the clinical model, these two models demonstrated a greater net benefit across a wide range of threshold probabilities in the external validation set, highlighting their improved decision-making value in clinical practice. Kaplan-Meier survival analysis revealed significant differences in recurrence-free survival (RFS) among the risk categories stratified by the nomogram across all subgroups, except for cases with small ccRCC tumors (≤ 4 cm). This suggests that while the nomogram effectively predicts recurrence, its performance remains limited in this specific subgroup. Furthermore, our findings indicate that the nomogram significantly outperforms the SSIGN model in predictive

performance. However, in the external validation cohort, the SSIGN model performed slightly better than the nomogram, although the difference was not statistically significant ($P>0.05$). Moreover, the nomogram can help identify low-risk patients within the intermediate-high risk SSIGN categories, thereby reducing unnecessary treatment for those unlikely to benefit from adjuvant therapy. Conversely, it can also detect high-risk patients within the low-risk SSIGN group who might otherwise be undertreated, ensuring the timely administration of adjuvant therapy to minimize recurrence risk. These findings highlight the incremental prognostic value of the nomogram and its potential as a valuable complement to existing prognostic models.

Using LASSO-Cox regression, we identified key radiomics features to construct a prognostic radiomics score, with each weighted feature capturing distinct aspects of tumor heterogeneity. In the intratumoral model, exponential_gldm_DependenceNonUniformity contributed the most. Here, "exponential" denotes an applied transformation, while the Gray Level Dependence Matrix (GLDM) quantifies spatial dependencies among gray-level values. A higher DependenceNonUniformity reflects greater textural heterogeneity. In the IPAT model, lbp_3D_k_glrlm_RunVariance emerged as the strongest predictor, characterizing spatial heterogeneity through run-length variance analysis of local binary pattern (LBP) filtered textures. These findings align with previous research linking radiomics heterogeneity to tumor invasiveness and prognosis [33].

Our study has several limitations. First, as a retrospective study, it is inherently subject to selection bias. Second, the two-center design and the relatively small external validation cohort may limit the generalizability of our findings, highlighting the need for multi-center studies with larger cohorts to enhance validation. Third, while the automated peritumoral expansion approach streamlines the workflow, it does not allow for a direct assessment of the prognostic value of the peritumoral region. Future studies should focus on delineating and analyzing this region separately to better understand its contribution. Fourth, our analysis was restricted to VOIs obtained from the arterial phase. Incorporating additional features extracted from other major CT phases, such as non-contrast and venous phases, may further improve the model's prognostic performance. Finally, although we have implemented measures such as reproducibility analysis, dual-observer segmentation, and image normalization to minimize technical variability, differences in scanning parameters and inter-patient variability may still impact the reproducibility of radiomic features.

Conclusion

The radiomics model and the fusion model, which integrate both intratumoral and peritumoral features, offer accurate prediction of recurrence risk in patients with localized ccRCC. These models have the potential to aid in personalized treatment planning, optimized surveillance strategies, and treatment strategies for patients with clear cell renal cell carcinoma.

Abbreviations

ccRCC	Clear cell renal cell carcinoma
RFS	Recurrence-free survival
IVS	Internal validation set
EVS	External validation set
ROI	Regions of interest
IAT	Internal area of the tumor
IPAT	Internal and peritumoral areas of the tumor
ICCs	Inter- and intra-observer and correlation coefficient
CPHR	Cox proportional hazards regression
LASSO	Least absolute shrinkage and selection operator
ROC	Receiver operating characteristic curve
FM	Fusion model
CM	Clinical model
RM	Radiomics model

Supplementary Information

The online version contains supplementary material available at https://doi.org/10.1186/s12880-025-01715-z.

Supplementary Material 1

Acknowledgements

Not applicable.

Author contributions

XL and YG conceived the project. XL, YG, FW, CD, and SH collected the data. XL analyzed the data; XL wrote the paper. JZ and DL revised this paper. All authors readed and approved the final manuscript.

Funding

The research reported in this publication was supported by the Scientific Research Project of Fujian for Youth (no. 2020QNB062 and no. 2020QNB061).

Data availability

The datasets generated and analyzed during the current study are not publicly available but are available from the corresponding author on reasonable request.

Declarations

Ethics approval and consent to participate

The study was conducted in accordance with the principles of the Declaration of Helsinki and approved by the institutional Ethics Committee in Zhongshan Hospital Fudan University, and the committee's reference number was B2021-608R.

Consent for publication

The need for written informed consent was waived with the confirmation of patient data confidentiality by the institutional Ethics Committee for this retrospective study.

Competing interests

The authors declare no competing interests.

Author details
[1]Department of Radiology, Zhongshan Hospital (Xiamen), Fudan University, Xiamen 361015, China
[2]Department of Radiology, Zhongshan Hospital, Fudan University, No 180, Fenglin Road, Xuhui District, Shanghai 200032, China
[3]Department of Medical Imaging, Xiamen Municipal Clinical Research Center for Medical Imaging, Xiamen 361015, China
[4]Department of Medical Imaging, Fujian Province Key Clinical Specialty for Medical Imaging, Xiamen 361015, China
[5]Department of Imaging Big Data and Artificial Intelligence, Xiamen Key Laboratory of Clinical Transformation of Imaging Big Data and Artificial Intelligence, Xiamen 361015, China
[6]Department of Urology, Zhongshan Hospital (Xiamen), Fudan University, Xiamen 361015, China

Received: 28 February 2024 / Accepted: 7 May 2025
Published online: 16 May 2025

References

1. Siegel RL, Miller KD, Jemal A. Cancer statistics, 2019. CA Cancer J Clin. 2019;69(1):7–34.
2. Capitanio U, Bensalah K, Bex A, et al. Epidemiology of renal cell carcinoma. Eur Urol. 2019;75(1):74–84.
3. Ravaud A, Motzer RJ, Pandha HS, et al. Adjuvant Sunitinib in High-Risk Renal-Cell carcinoma after nephrectomy. N Engl J Med. 2016;375(23):2246–54.
4. Martins F, Sofiya L, Sykiotis GP, et al. Adverse effects of immune-checkpoint inhibitors: epidemiology, management and surveillance. Nat Rev Clin Oncol. 2019;16(9):563–80.
5. Leibovich BC, Blute ML, Cheville JC, et al. Prediction of progression after radical nephrectomy for patients with clear cell renal cell carcinoma: a stratification tool for prospective clinical trials. Cancer. 2003;97(7):1663–71.
6. Sorbellini M, Kattan MW, Snyder ME, et al. A postoperative prognostic nomogram predicting recurrence for patients with conventional clear cell renal cell carcinoma. J Urol. 2005;173(1):48–51.
7. Correa AF, Jegede O, Haas NB, et al. Predicting renal Cancer recurrence: defining limitations of existing prognostic models with prospective Trial-Based validation. J Clin Oncol. 2019;37(23):2062–71.
8. Gillies RJ, Kinahan PE, Hricak H, Radiomics. Images are more than pictures. They Are Data Radiol. 2016;278(2):563–77.
9. Lambin P, Leijenaar RTH, Deist TM, et al. Radiomics: the Bridge between medical imaging and personalized medicine. Nat Rev Clin Oncol. 2017;14(12):749–62.
10. Jian L, Liu Y, Xie Y, Jiang S, Ye M, Lin HMRI. -Based radiomics and urine creatinine for the differentiation of renal Angiomyolipoma with minimal fat from renal cell carcinoma: A preliminary study. Front Oncol. 2022;12:876664.
11. Li X, Ma Q, Nie P, Zheng Y, Dong C, Xu W. A CT-based radiomics nomogram for differentiation of renal oncocytoma and chromophobe renal cell carcinoma with a central scar-matched study. Br J Radiol. 2022;95(1129):20210534.
12. Gao Y, Wang X, Wang S, et al. Differential diagnosis of type 1 and type 2 papillary renal cell carcinoma based on enhanced CT radiomics nomogram. Front Oncol. 2022;12:854979.
13. Hussain MA, Hamarneh G, Garbi R. Learnable image histograms-based deep radiomics for renal cell carcinoma grading and staging. Comput Med Imaging Graph. 2021;90:101924.
14. Demirjian NL, Varghese BA, Cen SY, et al. CT-based radiomics stratification of tumor grade and TNM stage of clear cell renal cell carcinoma. Eur Radiol. 2022;32(4):2552–63.
15. Zhou Z, Qian X, Hu J, et al. CT-based peritumoral radiomics signatures for malignancy grading of clear cell renal cell carcinoma. Abdom Radiol (NY). 2021;46(6):2690–8.
16. Xv Y, Lv F, Guo H, et al. Machine learning-based CT radiomics approach for predicting WHO/ISUP nuclear grade of clear cell renal cell carcinoma: an exploratory and comparative study. Insights Imaging. 2021;12(1):170.
17. Khodabakhshi Z, Amini M, Mostafaei S, et al. Overall survival prediction in renal cell carcinoma patients using computed tomography radiomic and clinical information. J Digit Imaging. 2021;34(5):1086–98.
18. Yan L, Yang G, Cui J, et al. Radiomics analysis of Contrast-Enhanced CT predicts survival in clear cell renal cell carcinoma. Front Oncol. 2021;11:671420.
19. Yang G, Nie P, Yan L, et al. The radiomics-based tumor heterogeneity adds incremental value to the existing prognostic models for predicting outcome in localized clear cell renal cell carcinoma: a multicenter study. Eur J Nucl Med Mol Imaging. 2022;49(8):2949–59.
20. Deniffel D, McAlpine K, Harder FN, et al. Predicting the recurrence risk of renal cell carcinoma after nephrectomy: potential role of CT-radiomics for adjuvant treatment decisions. Eur Radiol. 2023;33(8):5840–50.
21. Wang X, Zhao X, Li Q, et al. Can peritumoral radiomics increase the efficiency of the prediction for lymph node metastasis in clinical stage T1 lung adenocarcinoma on CT? Eur Radiol. 2019;29(11):6049–58.
22. Zhuo Y, Feng M, Yang S, et al. Radiomics nomograms of tumors and peritumoral regions for the preoperative prediction of spread through air spaces in lung adenocarcinoma. Transl Oncol. 2020;13(10):100820.
23. Jiang Y, Wang H, Wu J, et al. Noninvasive imaging evaluation of tumor immune microenvironment to predict outcomes in gastric cancer. Ann Oncol. 2020;31(6):760–8.
24. Shi J, Dong Y, Jiang W, et al. MRI-based peritumoral radiomics analysis for preoperative prediction of lymph node metastasis in early-stage cervical cancer: A multi-center study. Magn Reson Imaging. 2022;88:1–8.
25. Ma M, Gan L, Liu Y, et al. Radiomics features based on automatic segmented MRI images: prognostic biomarkers for triple-negative breast cancer treated with neoadjuvant chemotherapy. Eur J Radiol. 2022;146:110095.
26. Li X, Lin J, Qi H, et al. Radiomics predict the WHO/ISUP nuclear grade and survival in clear cell renal cell carcinoma. Insights Imaging. 2024;15(1):175.
27. Koo TK, Li MYA. Guideline of selecting and reporting intraclass correlation coefficients for reliability research. J Chiropr Med. 2016;15(2):155–63.
28. Shrout PE, Fleiss JL. Intraclass correlations: uses in assessing rater reliability. Psychol Bull. 1979;86(2):420–8.
29. Hu Y, Xie C, Yang H, et al. Assessment of intratumoral and peritumoral computed tomography radiomics for predicting pathological complete response to neoadjuvant chemoradiation in patients with esophageal squamous cell carcinoma. JAMA Netw Open. 2020;3(9):e2015927.
30. Zhang H, Yin F, Chen M, et al. Development and validation of a CT-Based radiomics nomogram for predicting postoperative Progression-Free survival in stage I-III renal cell carcinoma. Front Oncol. 2021;11:742547.
31. Kang B, Sun C, Gu H, et al. T1 stage clear cell renal cell carcinoma: A CT-Based radiomics nomogram to estimate the risk of recurrence and metastasis. Front Oncol. 2020;10:579619.
32. Zhang H, Yin F, Chen M, et al. [Predicting postoperative recurrence of stage I-II renal clear cell carcinoma based on preoperative CT radiomics feature nomogram]. Nan Fang Yi Ke Da Xue Xue Bao. 2021;41(9):1358–65.
33. Peeken JC, Shouman MA, Kroenke M, et al. A CT-based radiomics model to detect prostate cancer lymph node metastases in PSMA radioguided surgery patients. Eur J Nucl Med Mol Imaging. 2020;47(13):2968–77.

Publisher's note